Figure 5: *The Thorium-Argon spectrum. It may be compared with that given in the ESO Atlas of the Thorium-Argon Spectrum (ESO Scientific Report No. 6 – July 1987).*

On-line monitoring of centring errors, clouds, etc. is possible when the ratemeter is attached to the detector. Because the astronomer can see the spectrum building up, the object identification is obtained early in the observation, and integration can be halted when it is judged that a sufficiently high signal/noise ratio has been obtained. It is therefore very well suited to those problems in which very long exposures of faint objects are needed. Because there is no readout noise, long exposures can be broken into short segments that are interspersed with calibration spectra. This is a significant advantage for instruments, such as CASPEC, that suffer from flexure problems. For spectra taken with very high spectral

resolution, the rotation of the Earth smears long exposures. With the MAMA, long exposures of faint objects can be broken in order to obtain velocity calibrations. The MAMA has a very low dark background (about 0.1 event/pixel^{-1} hour^{-1} at 5C), and it also discriminates against the cosmic rays that plague long integrations with CCD detectors.

The ESO MAMA detector has a somewhat smaller ($\approx 1000 \times 250$ pixels) format than the CCDs and the loss of a number of pixels leaves one with only about 670×250 contiguous pixels. To achieve overlap of the spectral orders the short Camera must then be used. This results in a less than optimal mapping of a high resolution image onto the

relatively coarse resolution detector. If, in the future, the full MAMA format becomes available, the CASPEC Long Camera could be used and the detector pixel size would be better matched to the spectrograph optical resolution.

The present data taking software used with the MAMA does not allow access to IHAP during integrations. The computer is therefore not then available to perform other tasks, such as the precise estimation of the signal/noise ratio of an exposure as the integration proceeds, arithmetic on previous exposures, computing the continually changing atmospheric dispersion parameters, etc. The atmospheric dispersion parameters are needed to accurately centre the UV image of an object in the slit since the ESO TV cameras detect only the visual image of the object. Because the differential atmospheric dispersion is so large in the UV, the ability to calculate the position angle and amplitude of the dispersion is particularly important for a UV sensitive detector such as MAMA. Future minor revisions to the data taking software will allow the MAMA detector to be used more efficiently.

In conclusion, the ESO MAMA is a working detector with particular advantages for UV observations. A few minor modifications presently being undertaken will make the detector even easier to use. It thus fills a needed capability in the instrument compliment of ESO.

If there is sufficient user interest in the MAMA detector, ESO could purchase additional tubes with improved characteristics. We suppose that this will depend to some extent in the future availability of improved CCD detectors that could become competitive with the MAMA for the UV applications, as well as the interest in applications where the fast temporal response time of the MAMA can be utilized.

Deconvolution of NTT Images of E/S0 Galaxies

F. ZAVATTI[1], O. BENDINELLI[1], G. PARMEGGIANI[2], G. G. C. PALUMBO[1,4] and G. F. BIGNAMI[3]

[1] *Dipartimento di Astronomia, Università di Bologna, Italy.*
[2] *Osservatorio Astronomico di Bologna, Italy.*
[3] *I. F. C. T. R./C. N. R., Milano, Italy.*
[4] *I. TE. S. RE./C. N. R., Bologna, Italy.*

Introduction

The New Technology Telescope (NTT) has recently become fully operational and subsequently made available by ESO to European astronomers in the standard scheduling procedure.

The first glimpses of the high quality images obtainable by virtue of the happy combination of advanced technology and excellent seeing conditions at La Silla have already been published (*The Messenger,* issues 56 and 58).

On the other hand, in recent years a considerable effort has been put into the development of highly sophisticated mathematical techniques to deconvolve images in one and two dimensions.

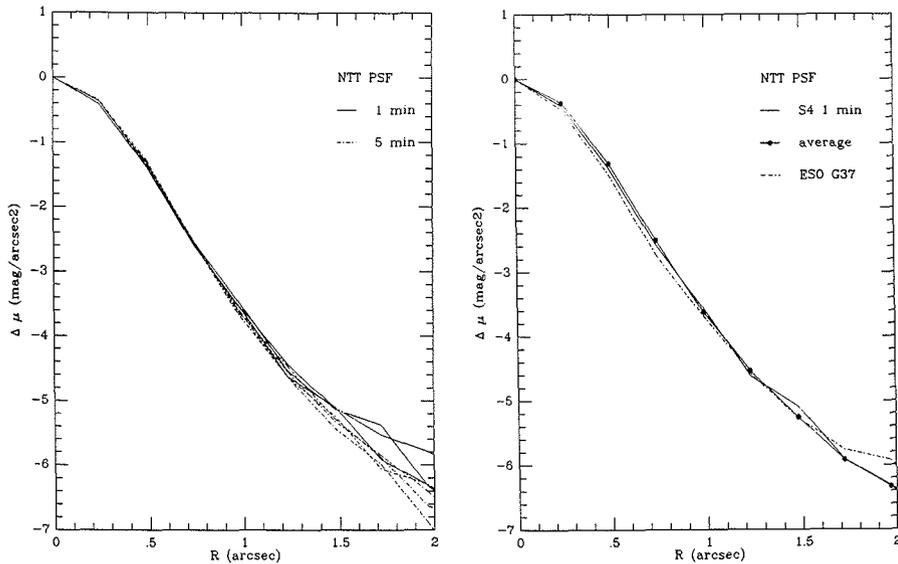Although the effects of atmospheric

Figure 1: *(a) Brightness profiles of some stars near PKS 1209-52 from 5 and 1 minute integration time. (b) Brightness profile of the adopted (average) PSF (solid circles and line) compared with the one of the most luminous star in the 1-minute frame (solid line). The dashed line is the PSF derived from a star in the ESO 440 G 37 frame.*

turbulence which produces image blurring cannot entirely be abolished in any image taken with a ground-based telescope, one can aim, deconvolving with the Point Spread Function (PSF), at "cleaning" the observed image in order to approximate the "real" image, as it would be obtained in the absence of the atmosphere. This process has been applied on various occasions using a variety of deconvolution techniques and has been proven to be quite powerful. There still is a debate, however, on which mathematical technique works best. Combining high quality images with robust deconvolution processes, one can hope to reach a better understanding of both the relative power of the algorithms used and the goodness of the images obtained, or, in turn, to test the telescope characteristics.

During the first general observer NTT run, a few images of well-known bright galaxies were obtained in good seeing conditions by one of us (G.F.B.).

The present paper describes the observation of those objects and the three mathematical algorithms used to deconvolve their images. From the results obtained, conclusions can be drawn on the relative power of the deconvolution techniques used, the quality of the images the NTT is able to acquire and some interesting astrophysical aspects of the objects studied.

Observations

Five E/S0 galaxies: ESO 440 G 37, NGC 3115, NGC 3585, NGC 3904, NGC 3923 were observed. These images were obtained using the RCA # 15 CCD cam-

era (515 × 313 pixels; Nasmyth focus) at the ESO NTT telescope in the V band. The images were acquired on the night of January 24, 1990. The typical seeing FWHM was 0.68 arcsec for the duration of these observations, and the sampling was 0.246 arcsec/pixel (rebinned images). A total of eight CCD frames were obtained with integration times ranging from 25 to 210 sec. Standard processing of frames for flat field and bias was used. In this note we discuss the deconvolution of these elliptical galaxies.

The Point Spread Function

Star images suitable for PSF extraction were not available in all frames. Two frames of the stellar field near PKS 1209-52 (1 and 5 minutes exposure time) were therefore used in order to derive an average PSF. Such Point Spread Function was used for deconvolving all extended objects in the present sample. The seeing conditions for this reference star field were monitored to be identical to those of the galaxy images.

The stability of the star profiles can be deduced from Figure 1 a, where some stars from both 1 and 5 minutes ex-

posures are shown, and from Figure 1 b where the adopted average PSF from the 5-minute frame is compared with the most luminous star in the 1-minute exposure image as well as with a star in the field of the galaxy ESO 440 G 37.

The average PSF (HWHM ~ 0.34 arcsec) was fitted with a sum of 3 Gaussians (e.g. Bendinelli et al., 1987, 1989) as well as a Moffat (1969) function; the fit parameters are listed in Table I.

This comparison brings the conclusion that the NTT and the seeing conditions were considerably stable both within each single frame and from one frame to another.

The Deconvolution

Surface brightness profiles were extracted using the VISTA code.

All galaxies in our sample were deconvolved by means of three quite different techniques:

– Regularized numerical inversion of the convolution integral equation (RLS), applied to brightness profiles. Such method was previously used in the deconvolution of a variety of very different objects (see e.g. Bendinelli et al., 1986 and references therein). With a PSF expressed in terms of Moffat function.

– Regularized Multi-Gaussian (RMG), based on the analytical solution of the convolution integral equation when both object and PSF are expressed as a sum of Gaussian functions.

This method has two major advantages:

(a) it is insensitive to undersampling

(b) it runs a whole deconvolution cycle in a few seconds on a Personal Computer.

The major limitation of the RMG method, however, is that it is applicable only to round or elliptical images and does not work on images lacking symmetry.

– Deconvolution adopting a method devised by Hunt (1973) (HUNT). This is a bidimensional deconvolution and makes use of FFT, and basically is a generalization of Wiener's filter. As far as we are aware the HUNT method has only been applied to astronomical images once by Heap and Linder (1987) for deconvolving the image of SN 1987 A.

The three deconvolution methods

TABLE I: *Parameters of the fitted average PSF*

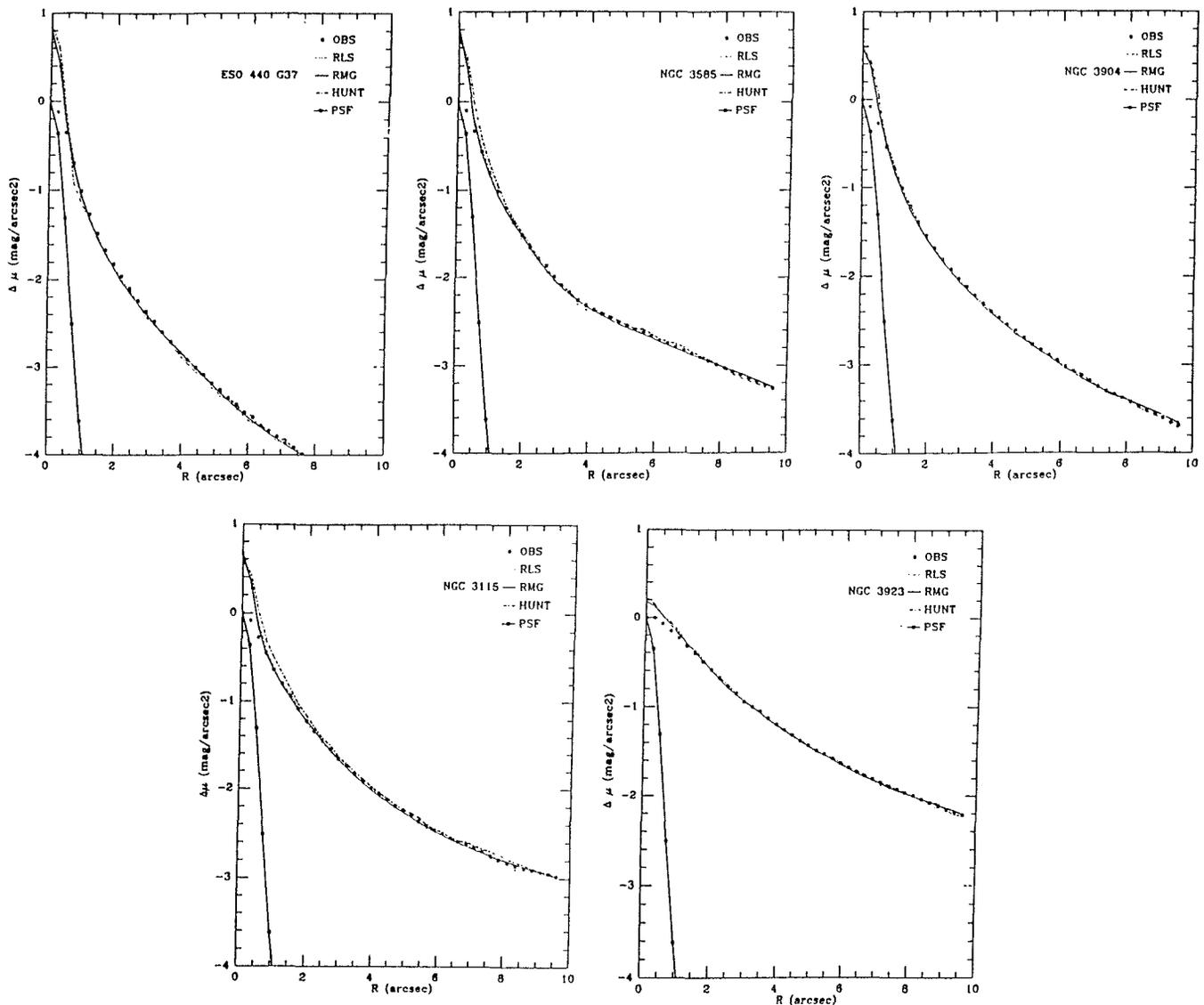| FWHM (arcsec)	3-Gaussian fit L_i, σ_i, i = 1, 2, 3		Moffat fit α, β	
0.68	0.572 0.306 0.115	0.290 0.518 1.121	0.504	2.195
Note: σ_i, α in arcsec.				

Figure 2: *Observed (solid dots) and deconvolved (lines) profiles of the five galaxies. Observed PSF profiles, normalized to the central brightness of the galaxies, are also shown as solid lines and dots.*

listed above are compared on the same image here for the first time although the first two (RLS and RMG) were discussed in Bendinelli et al. (1990).

Table II gives some of the relevant parameters of the deconvolutions: observed and deconvolved HWHM, in arcsec, for the different methods and the difference in observed and deconvolved central surface brightness.

If a *gain in resolution* is defined as the ratio between the HWHM of the observed and deconvolved profiles, then from this table values can be derived ranging from 1.3 to 3.7, depending on the relative dimension of galaxy and PSF.

In Figure 2 observed and deconvolved profiles of the five galaxies are presented.

The results do not depend on the functional form choosen for the PSF representation, confirming previous tests (Bendinelli et al., 1988).

Discussion of the Results

Table II should be regarded as the main result of this work which goes toward the analysis of core structure of early type galaxies, as outlined in Bendinelli et al. (1990).

Differences among the deconvolution methods are of the order of some per cent, small enough to justify the state-

ment that with these images (i.e. pixel size, object size, PSF) all three methods work equally well.

This means that the unambiguous identification of a "point" mass in the centre of nearby galaxies, if present, is possible by a variety of methods, if well-sampled data are available. This central mass concentration with higher mass-to-light ratio than the stars that appear

TABLE II: *Parameters of the deconvolved profiles*

Galaxy	OBS	RLS		RMG		HUNT	
	HWHM	HWHM	$\Delta\mu$	HWHM	$\Delta\mu$	HWHM	$\Delta\mu$
E 440 G 37	0.75	0.42	0.73	0.38	0.80	0.40	0.86
NGC 3585	0.88	0.40	0.71	0.24	0.82	0.49	0.70
NGC 3904	0.90	0.52	0.59	0.50	0.59	0.57	0.58
NGC 3115	1.07	0.48	0.60	0.43	0.66	0.58	0.60
NGC 3923	2.27	1.80	0.18	1.80	0.18	1.74	0.22

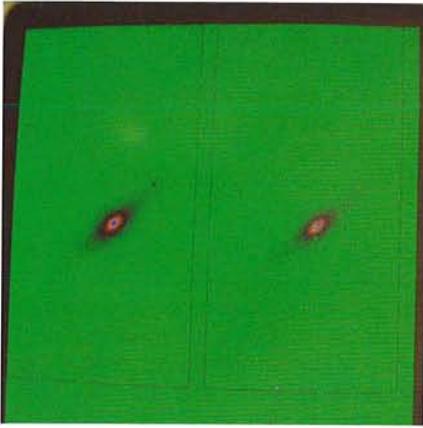Note: HWHM in arcsec; $\Delta\mu$ = (observed-deconvolved) in mag/arcsec^2.

Figure 3: *NGC 3115-S0 galaxy; $B_T = 9.75$. Left panel: original CCD frame (1.7×0.9). Right panel: Hunt deconvolution.*

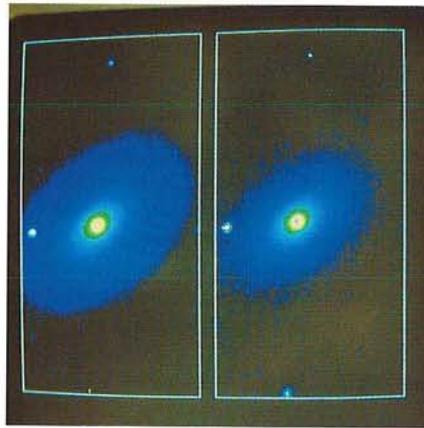Figure 4: *NGC 3585, also ESO 502 G 25−E galaxy; $B_0 = 11.40$. Left panel: original CCD frame (1.7×0.9). Right panel: Hunt deconvolution.*
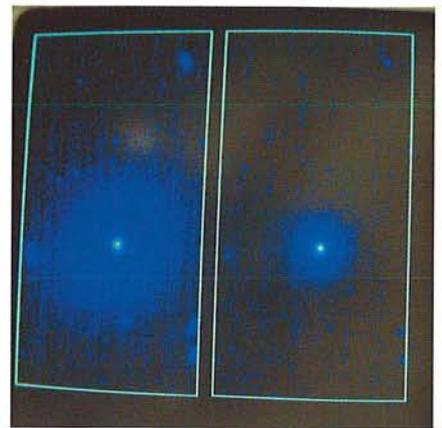

Figure 5: *ESO 440 G 37−E-S0 galaxy; $B_0 = 14.30$. Left panel: original CCD frame (1.7×0.9). Right panel: Hunt deconvolution.*

to dominate in any tested object the galaxy mass distribution on scales of tens to hundreds of parsec has tentatively been identified with a black hole by many authors.

The debate on the presence of black holes in the centre of galaxies is still quite open since the data seem only to imply that some additional mass is required on rather small scales in the centre of galaxies.

Hence any deconvolution method which will permit to constrain the mass distribution in the core of galaxies may be regarded as a step forward towards the understanding of galaxies themselves and the existence of black holes in their centres.

This work was supported in part by the Ministero della Pubblica Istruzione and Osservatorio Astronomico di Bologna.

References

Bendinelli, O., Parmeggiani, G., and Zavatti, F.: 1986, *Ap. J.* **308**, 611.

Bendinelli, O., Parmeggiani, G., Piccioni, A., and Zavatti, F.: 1987, *Astron. J.* **94**, 1095.

Bendinelli, O., Parmeggiani, G., and Zavatti, F.: 1988, *J. Astrophys. Astron.* **9**, 17.

Bendinelli, O., Parmeggiani, G., and Zavatti, F.: 1989, in *Highlights of Astronomy*, proc. 20th IAU General Assembly, in press. Dordrecht: Kluwer.

Bendinelli, O., Parmeggiani, G., Zavatti, F., and Djorgovski, S.: 1990, *Astron. J.* **99**, 774.

Gouiffes, G., Wampler, E.J., Baade D., and Wang, L.-F.: *The Messenger*, **58**, 11.

Heap, S.R., and Linder, D.J.: 1987, *Astron. Astrophys.* **185**, L10.

Hunt, B.R.: 1973, *IEEE Trans. Comp.*, **C-22**, 805.

Moffat, A.F.J.: 1969, *Astr. Ap.*, **3**, 455.

MIDAS Memo

ESO Image Processing Group

1. Application Developments

The main efforts were placed on validation of basic MIDAS commands and the subsequent correction of problems reported. Since the next major release 90 NOV will be frozen in September already, only a limited number of these improvements will be available in that release.

The COPY/DISPLAY command which can produce hard copies of the image display has been upgraded to be able to provide output for colour PostScript printers. This makes it possible to get good working hard copies in both B/W and colour directly from the image display in MIDAS.

2. New Positions

Two additional short-term positions (with durations of up to two years) have been allocated to the MIDAS group. They will be used mainly for improvements and developments of new application programmes in MIDAS. Not only will this make it possible to have new algorithms and applications included into MIDAS after a period of limited improvements in this area, but will spread long-term, detailed knowledge of MIDAS in the community when people in these positions return to their home institutes.

In addition to these positions, it will be possible to invite people who have made interesting algorithms and programmes, to ESO for an implementation of them into the MIDAS environment. People interested in contributing and/or making new applications to MIDAS may contact the IPG with detailed descriptions.

3. Distribution Policy

The ESO Council, during its last meeting in June 1990, defined the policy for usage and distribution of MIDAS. It states that MIDAS is the image processing system of ESO to be used both for off-line data reductions and for on-line evaluation of data from ESO telescopes including the VLT. MIDAS is available to all non-profit research organizations. Such organizations must sign a User Agreement with ESO before obtaining the package. This agreement will regulate the usage of MIDAS and ensure that it is not exploited commercially. This policy will be implemented as of the 90 NOV release of MIDAS.

4. MIDAS on New Systems

The 90 MAY release of MIDAS was installed on an IBM System 6000 Model 540 (the new RISC CPU) made available by IBM. Only very minor problems were detected, all relating to the operating system AIX 3.1 which was a preliminary version during the tests. Those problems have been resolved in the official release of AIX 3.1. The system had an